

# Maximum Torque Per Ampere and Flux-weakening Control for PMSM Based on Curve Fitting

Shoudao Huang  
College of electrical and information engineering  
Hunan University  
Changsha China  
shoudaohuang@tom.com

Ziqiang Chen  
College of electrical and information engineering  
Hunan University  
Changsha China  
chzq1986@163.com

Keyuan Huang  
College of electrical and information engineering  
Hunan University  
Changsha China  
kyhuang@163.com

Jian Gao  
College of electrical and information engineering  
Hunan University  
Changsha China  
gj\_2520596@sina.com.cn

**Abstract**-This paper describes the MTPA (maximum torque per ampere) control strategy of Salient-pole PMSM (permanent magnet synchronous motor) and its flux-weakening control strategy. Salient-pole PMSM often used the MTPA control strategy, the method that MTPA curves obtained from look-up table is usually used, but it will reduce the real-time performance and reliability of the system. In this paper, electromagnetic torque  $T_{em}$  and the relationship of the AC-DC-axis currents  $i_d, i_q$  can be derived with the curve fitting method directly. It approximates the original nonlinear equations into a set of two-dimensional linear equation, and the error analysis shows that the error in line with engineering requirements, so it is greatly simplifies and facilitates the actual operation. On this basis, the paper also introduces the phase-shifting controlled manner to achieve flux-weakening control. The control performance of motor with improved algorithm is analyzed through simulation, and the simulation results verify the validity and feasibility of the algorithm and theory.

## I. INTRODUCTION

Salient-pole PMSM (permanent magnet synchronous motor) often used the MTPA (maximum torque per ampere) control strategy[1]-[4], i.e. the per unit current output of the maximum torque, while the relationship between the electromagnetic torque  $T_{em}$  and the AC-DC-axis currents  $i_d, i_q$  are non-linear equations, solving these equations are difficult, especially in the use of digital control of the microcomputer chip. The usual approach is to use look-up table, i.e. from the known electromagnetic torque  $T_{em}$ , through the relationship between  $T_{em}$  and  $i_d, i_q$ , solving a corresponding  $i_d, i_q$ , and then make a table with the corresponding values, in actual operation, the needed  $i_d, i_q$  can be obtained by look-up table from a given  $T_{em}$ .

But the look-up table method increase the system's computing burden for the digital system, the system takes a lot of time for data query, thus reducing the real-time performance and reliability of the system. In this paper, a method of two-dimensional curve fitting is proposed, which fit the corresponding data into a group of two-dimensional linear equation, within the permitted error ranges, the digital system obtain the  $i_d, i_q$  value by the way of real-time calculation of two-dimensional linear equations, thus, the method can significantly save computing time and improving

system real-time performance and reliability.

Based on the above, this paper goes on with the way of using phase-shifting to achieve flux-weakening control for the salient-pole PMSM[5]-[9]. The simulation results verify the validity and feasibility of the algorithm and theory.

## II. MTPA CONTROL STRATEGY

Implicit-pole PMSM's MTPA control trajectory is the q-axis, therefore, for the implicit-pole PMSM, the MTPA control is  $i_d = 0$  control. Because of the salient-pole motor existence of salient-pole effect, MTPA trajectory is not the same.

When stable operation of a PMSM, the electromagnetic torque can be expressed as:

$$T_{em} = 1.5p[\psi_f i_q + (L_d - L_q)i_d i_q] \quad (1)$$

Equation (1) could be expressed in per-unit value form as:

$$T_{em}^* = 1.5i_q^*(1 - i_d^*) \quad (2)$$

where  $i_b$  is the current base value:  $i_b = \psi_f / (L_q - L_d)$ ,  $T_b$  is the torque base value:  $T_b = p\psi_f i_b$ ,  $p$  is the pole pair number,  $\psi_f$  is the magnet flux,  $i_d$  and  $i_q$  are d-axis and q-axis current components respectively,  $L_d$  and  $L_q$  are d-axis and q-axis inductance components respectively.

When using the MTPA control strategy, the motor current vector should be satisfied:

$$\begin{cases} \frac{\partial(T_{em} / i_s)}{\partial i_d} = 0 \\ \frac{\partial(T_{em} / i_s)}{\partial i_q} = 0 \end{cases} \quad (3)$$

where  $i_s$  is the stator current, substituting (1) and  $i_s = \sqrt{i_d^2 + i_q^2}$  into (3),  $i_d$  can be obtained:

$$i_d = \frac{-\psi_f + \sqrt{\psi_f^2 + 4(L_d - L_q)^2 i_q^2}}{2(L_d - L_q)} \quad (4)$$

Equation (4) could be expressed in per-unit value form as:

$$i_d^* = \frac{1 - \sqrt{1 + 4i_q^{*2}}}{2} \quad (5)$$

Substituting (5) into (2), we can get the relationship between AC-DC-axis current components and electromagnetic torque:

$$\begin{cases} T_{em}^* = 1.5\sqrt{-i_d^*(1-i_d^*)^3} \\ T_{em}^* = 0.75i_q^*[1 + \sqrt{1 + 4i_q^{*2}}] \end{cases} \quad (6)$$

In turn, then the stator current components  $i_d^*$  and  $i_q^*$  can be expressed as:

$$\begin{cases} i_d^* = f_1(T_{em}^*) \\ i_q^* = f_2(T_{em}^*) \end{cases} \quad (7)$$

For any given torque, according to (6), two components of the minimum current as the current control command value can be obtained to achieve the MTPA control of the motor.

#### A. Maximum torque per ampere control realization

Equation (6) are non-linear equations, requiring solution of these equations are difficult, which caused inconvenience to the specific operations, commonly used the look-up table method to achieve in digital systems. Through observation and experiment, (6) can be replaced approximately by a group of two-dimensional linear equations through curve fitting.

A set of corresponding data,  $T_{em}^*$  and  $i_d^*$  in (6), could be calculated by using dichotomy method,  $T_{em}^*$  will be limited to (0,3), while the actual maximum value will up to 2 ~ 3, step length of  $T_{em}^*$  can be taken as 0.05, we can get 60 sets of data in the following Table I :

TABLE I. A set of corresponding data,  $T_{em}^*$  and  $i_d^*$

$T_{em}^*$	$i_d^*$	$T_{em}^*$	$i_d^*$
0.05	-0.0011	1.55	-0.3941
0.1	-0.0044	1.6	-0.4078
0.15	-0.0097	1.65	-0.4214
0.2	-0.0169	1.7	-0.4348
0.25	-0.0257	1.75	-0.4482
0.3	-0.036	1.8	-0.4614
0.35	-0.0474	1.85	-0.4745
0.4	-0.0598	1.9	-0.4875
0.45	-0.0729	1.95	-0.5004
0.5	-0.0866	2	-0.5131
0.55	-0.1088	2.05	-0.5258
0.6	-0.1153	2.1	-0.5384
0.65	-0.1301	2.15	-0.5508
0.7	-0.145	2.2	-0.5632
0.75	-0.1601	2.25	-0.5754
0.8	-0.1753	2.3	-0.5876
0.85	-0.1904	2.35	-0.5996
0.9	-0.2055	2.4	-0.6116

0.95	-0.2206	2.45	-0.6235
1	-0.2356	2.5	-0.6353
1.05	-0.2505	2.55	-0.6469
1.1	-0.2654	2.6	-0.6585
1.15	-0.2802	2.65	-0.6701
1.2	-0.2948	2.7	-0.6815
1.25	-0.3094	2.75	-0.6928
1.3	-0.3238	2.8	-0.7041
1.35	-0.3381	2.85	-0.7152
1.4	-0.3523	2.9	-0.7264
1.45	-0.3663	2.95	-0.7374
1.5	-0.3803	3	-0.7484

Through the MATLAB two-dimensional curve fitting function polyfit() fitted out the two-dimensional linear equation of  $T_{em}^*$  and  $i_d^*$  as follows[10]:

$$i_d^* = 0.01*T_{em}^{*2} - 0.298*T_{em}^* + 0.0481 \quad (8)$$

In the above equation, although when the  $T_{em}^* = 0$ ,  $i_d^*$  is not 0, whether no-load start or start with a set,  $T_{em}^*$  is not 0, therefore, when the actual operation will not be the case  $T_{em}^* = 0$ , this is the reason why the table  $T_{em}^*$  does't start from 0.

Substituting (8) into (2), we can get the relationship between  $T_{em}^*$  and  $i_q^*$ :

$$i_q^* = -\frac{2}{3} * \frac{T_{em}^*}{0.01*T_{em}^{*2} - 0.298*T_{em}^* + 0.9519} \quad (9)$$

Equation (8) and (9) is calculated according to (6), due to (6) has general availability, so (8) and (9), also has general availability.

#### B. Error analysis

Make the difference calculation between the actual curve of Table I and the fitting curve  $i_d^* = f_1(T_{em}^*)$  of (8), the two curves and the error curve in the form of graphically described as shown in Figure 1 and Figure 2. Figure 1, solid

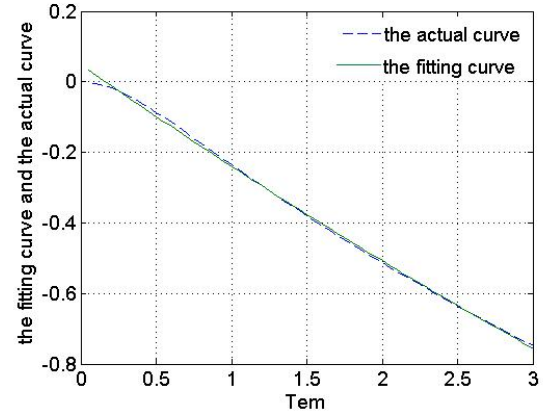


Figure 1. The fitting curve and the actual curve

line shows the fitting curve and dotted line represents the actual curve, we can see that the two curves is extremely close. Figure 6 is the error map of the difference between the actual value and the fitted value. As can be seen, the

maximum error is only 3.5%, and this time corresponds to the situation when the motor in no-load, when the motor runs in full load ,  $T_{em}$  is about 0.67, and the error is only 1%.

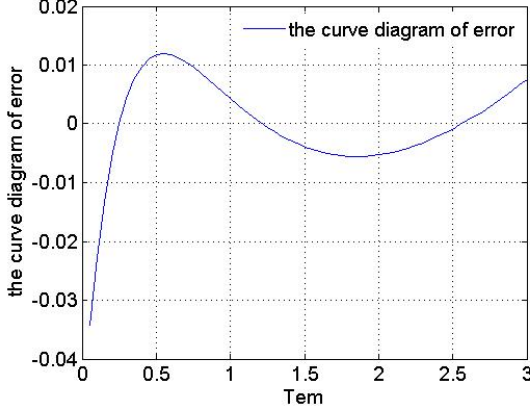


Figure 2. The curve diagram of error

### C. Maximum torque per ampere controller design

According to the method above, the control block diagram for the system is shown in Fig3, a given speed  $\omega^*$  comparison with the actual speed  $\omega_r$ , after regulation of speed loop, output torque command given value  $T_{em}^*$ ,  $T_{em}^*$  pass through (8) and (9) and calculate the given value  $i_d^*$  and  $i_q^*$  of the AC-DC axis current, and then after regulation of current loop, output of the AC-DC axis voltage, finally, obtained the stationary axis voltage which is required for modulation by rotation transformation.

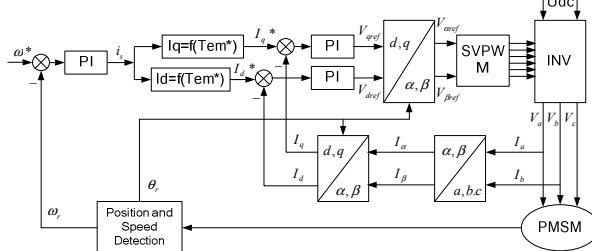


Figure 3. Salient-pole PMSM MTPA control system diagram.

## III. FLUX-WEAKENING CONTROL FOR PMSM

The voltage equation of a PMSM can be expressed as:

$$u = \omega \sqrt{(\rho L_d i_q)^2 + (L_d i_d + \psi_f)^2} \quad (10)$$

Where  $u$  is the stator voltage,  $\omega$  is the electrical angular velocity,  $\rho$  is the salient-pole rate of the motor. As can be seen from (10), the motor speed is proportional to the terminal voltage of PMSM, so when the motor reached rated speed, in order to further improve the speed, while maintaining the motor terminal voltage constant , only by regulating  $i_d$ ,  $i_q$ , which is so-called flux-weakening control ,

usually through increasing the direct-axis demagnetization current to achieve.

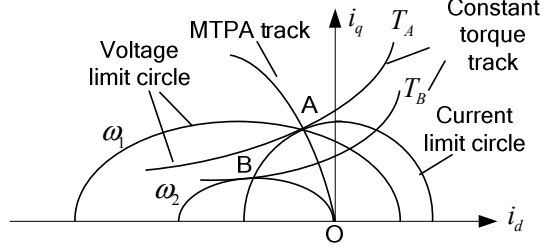


Figure 4. Stator current vector track.

The flux-weakening speed control for PMSM can be illustrated by the stator current vector trajectory as shown in Fig.4. First, the motor run along with OA, the MTPA curve. When the motor voltage and current reached the limit, the time the speed  $\omega_1$  corresponding to the turning speed when the motor reach maximum torque  $T_A$ . To further increase speed to  $\omega_2$ , while making maximum use of inverter capacity, it is need to control the current vector to run along the current limit circle, i.e. counter-clockwise down along the AB segment. As can be seen from the diagram, when the current vector run from point A to point B, the direct-axis demagnetization current component increases, at the same time , the motor output torque smaller, i.e. constant power operation[11][12].

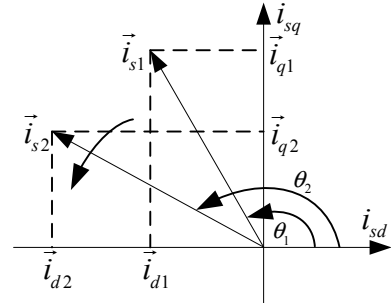


Figure 5. Phase-shifting flux-weakening control current vector graph.

In this paper, the flux-weakening control algorithm is phase-shifting, as shown in Fig.5, when the current vector is  $\vec{i}_{s1}$ , if the time the motor's speed  $\omega_1$  corresponding to the turning speed when the motor reach maximum torque, in order to achieve flux-weakening, i.e. increase the direct-axis demagnetization current component  $i_d$ , the angle  $\theta_1$  corresponding to  $i_{s1}$  can be increased to angle  $\theta_2$ , at this time  $i_{s1}$  becomes  $i_{s2}$ . From the figure we can see that after phase-shifting the direct-axis flux-weakening current component increased.

In order to achieve phase-shifting flux-weakening control, we need to find a flux-weakening adjustment coefficient, the coefficient can be calculated according to:

$$M = \frac{\sqrt{3} \sqrt{u_{sd}^2 + u_{sq}^2}}{U_{dc}} \quad (11)$$

Where  $u_{sd}$  and  $u_{sq}$  are d-axis and q-axis voltage components respectively,  $U_{dc}$  is the DC bus voltage.

Phase-shifting flux-weakening control system block diagram shown in Fig.6, The error obtained by comparing the actual measured adjustment coefficient  $M$  with the setting  $M^*$ , outputs the given value of the angle through the flux-weakening loop adjustment. When the difference is less than 0, the angle outputted by flux-weakening loop unchanged. When the difference is greater than 0, the angle outputted by flux-weakening loop increased, i.e. the system is turned to flux-weakening control. It should be noted that the flux-weakening loop is a pure integrator, and in order to prevent integrator saturation, the setting value of adjustment coefficient can get close to 1.

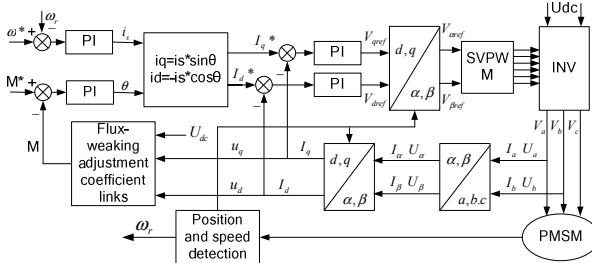


Figure 6. Phase-shift flux-weakening control system diagram.

Should be pointed out that when the system from the MTPA control transition to flux-weakening control, it is need to combine these two parts above-mentioned, i.e. Fig.3 and Fig.6 combined.

#### IV. SIMULATION RESULTS AND ANALYSIS

Simulation model is established under MATLAB environment using simulink tool box. The PMSM is used for electric vehicles, its parameters can be seen in Table II and the simulation curve can be seen in Fig.7-10. In graph, maximum current limiting is about twice as rated current, i.e. 180A, maximum torque limiting is three times as rated torque, namely 120N.m.

TABLE II. Motor parameters

Number of pole pairs	4
Rated speed	1500r/min
Sensing line voltage RMS	36V
Rated line current	96A
Rated torque	40N.m
Rated power	6.3kW
Cross-axis inductance	0.2828mH
Direct-axis inductance	0.1346mH
Phase winding resistance	0.0115ohm

Fig.7 presents simulation waveform when MTPA control with no load. AC-DC-axis current  $i_d$ ,  $i_q$  is the corresponding output according to torque  $T_{em}$  input based on fitting curve. By calculation, the error between the optimal  $i_d$ ,  $i_q$  obtained by fitting curve and actual optimal value in the experiment is not exceeded 3%. The fitting curve would be more accurate and have less error if more corresponding data,  $T_{em}^*$  and  $i_d^*$  have been sampled.

Fig.8 stands for simulation waveform when MTPA control with full load. AC-DC-axis current would be operate optimally whether it is in start-up condition or in stable operation.

Fig.9 is no-load simulation waveform when system is start-up by MTPA control to flux-weakening control. The test only achieves one-time rated speed in flux-weakening operation, namely 3000r/min. As it can be seen from the graph, stator current would reach its rated value when motor speed is up to 3000r/min even if operate in no-load condition.

Fig.10 is full-load simulation waveform when system is start-up by MTPA control to flux-weakening control. As it can be reflected from top left picture, demagnetization current component  $i_d$  is accounting for 35% in MTPA control while in flux-weakening control, demagnetization current component  $i_d$  is accounting for 80%. However, as can be seen from top right picture, stator current has not increased continuously, keeping stable around rated current value owing to current limiting circle constraints. Below left picture of electromagnetic torque simulation waveform shows that when motor operates in rated condition, system

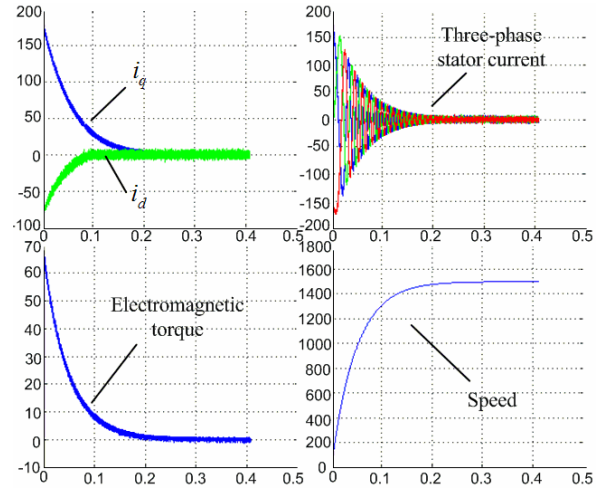


Figure 7. No-load waveforms of MTPA control.

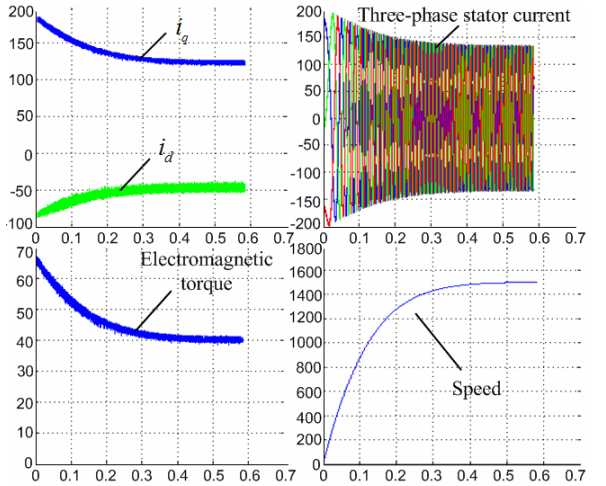


Figure 8. Full-load waveforms of MTPA control.

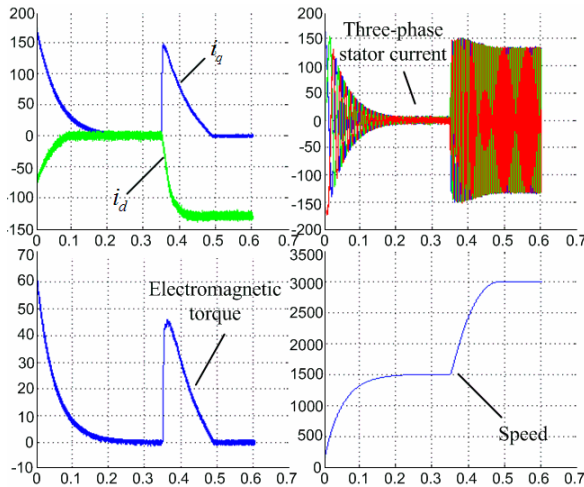


Figure 9. No-load waveforms of MTPA control switch to flux-weakening control.

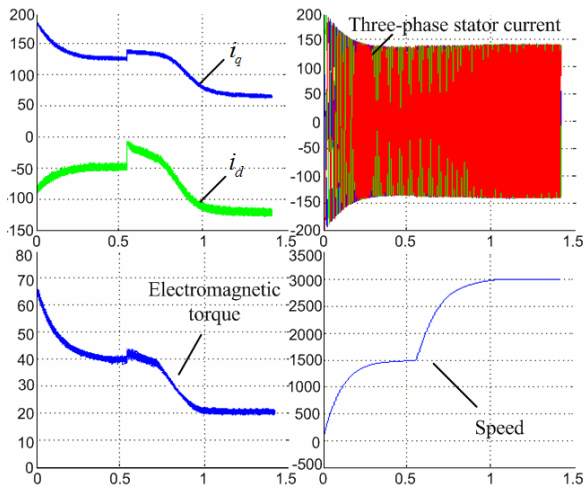


Figure 10. Full-load waveforms of MTPA control switch to flux-weakening control.

carried out flux-weakening control. Electromagnetic torque will decrease as rotational speed increases. It would decrease to 20N.m when motor keep stable operation at 3000r/min. Motor keeps in constant power operation in whole flux-weakening control.

Both figures show very close correlation with the algorithm and theory.

## V. CONCLUSIONS

A kind of MTPA control strategy of salient-pole PMSM which used in electric vehicles is proposed in this paper, according to data relation between torque and AC-DC-axis

current, original nonlinear equation is fitted to two-dimensional linear equations by adopting curve fitting. On this basis, the motor flux-weakening control using phase-shifting method is also proposed in the paper. When motor is in MTPA control, it operates in optimum current way. However, when motor adopts flux-weakening control, it operates in constant power way. It can be seen from the simulation waveform that whether MTPA control or flux-weakening control can verify the validity and feasibility of the proposed method. Therefore, the method has provided design basis for the engineering practice, possessing guiding significance.

## REFERENCES

- [1] Ren Yuan Tang, "Modern permanent magnet machines theory and design," Beijing:Machinery Industry Press, 2005.
- [2] Yan Ping Xu, Yan Ru Zhong, "Simulation of minimum loss control for PMSM," Journal of System Simulation, vol. 19, pp. 5283-5286, Dec 2007.
- [3] Bolognani S, Petrella R, Prearo A, Sgarbossa L, "Automatic tracking of MTPA trajectory in IPM motor drives based on AC current injection," Energy Conversion Congress and Exposition (ECCE 2004), Sept 2004, pp.2340-2346.
- [4] Consoli A, Scarcella G, Scelba G, Testa A, "Steady-state and transient operation of ipmsm under maximum-torque-per-ampere control," IEEE Trans. on Industry Applications, vol. 46, pp.121-129, Feb 2010.
- [5] Hai Yan Liu, Yi Wang, Jie Liu, Chang Liu, "Field-weakening control of induction motor for electric vehicles," Electric Machines and Control, vol. 9, pp. 452-455, Sep 2005.
- [6] Tao Zhou, Qing Liang Liu, "Flux-weakening method for permanent magnet synchronous motor by lead-angle control," Appliance Technology, 2003, pp.61-64.
- [7] Yi Wang, Hong Fei Ma, Kai qi Zhao, Dian Guo Xu, et al, "Field-oriented vector control of induction motor for electric vehicles," Proceedings of the Csee, vol. 25, pp. 115-119, June 2005.
- [8] Y. S. Kim, Y. K. Choi, J. H. Lee, "Speed-sensorless vector control for permanent-magnet synchronous motors based on instantaneous reactive power in the wide-speed region," IEEE Proc-Electr. Power Appl., vol. 152, pp. 1343-1349, Sept 2005.
- [9] Morimoto S, Takeda Y, Hirasa T, Taniguchi K, "Expansion of operating limits for permanent magnet motor by current vector control considering inverter capacity," IEEE Tran. on Ind. Application, vol. 26, pp. 886-871, Sept/Oct 1990.
- [10] Ping Zhang, "Concise guide to MATLAB gundamentals and applications," Beijing:Beijing University of Aeronautics and Astronautics Press, 2001.
- [11] Schiferl RF, Lipo TA, "Power capability of salient pole permanent magnet synchronous motor in variable speed drive applications," IEEE Trans. Ind. Application, vol. 26, pp. 115-123, Jan/Feb 1990.
- [12] Morimoto S, Sanada M, Takeda Y, "Inverter-driven synchronous motor for constant power," IEEE Ind. Appl. Magazine, vol. 2, pp. 18-24, Nov/Dec 1996.